

1
2
3
4
5
6
7
8
9
10
11
12
13
14
15
16
17
18
19
20
21
22
23
24
25
26
27
28
29

Cortical microstructure and hemispheric specialization – a diffusion-imaging analysis in younger and older adults

Paweł P. Wróbel, MD^{1*}, Hanna Braaß, MD¹, Benedikt M. Frey, MD¹, Marlene Bönstrup, MD², Stephanie Guder, MD¹, Lukas K. Frontzkowski, MD¹, Jan F. Feldheim, MS¹, Bastian Cheng, MD¹, Yogesh Rathi, PhD^{3,4}, Ofer Pasternak, PhD^{3,4}, Götz Thomalla, MD¹, Inga K. Koerte, MD PhD^{3,5,6}, Martha E. Shenton, PhD^{3,4,6}, Christian Gerloff, MD¹, Fanny Quandt, MD¹, Focko L. Higgen, MD^{1#}, Robert Schulz, MD^{1#}

¹ Department of Neurology, University Medical Center Hamburg-Eppendorf, Hamburg, Germany

² Department of Neurology, University Medical Center, Leipzig, Germany

³ Psychiatry Neuroimaging Laboratory, Brigham and Women's Hospital, Harvard Medical School, Boston, USA

⁴ Department of Radiology, Brigham and Women's Hospital, Harvard Medical School, Boston, USA

⁵ cBRAIN, Department of Child and Adolescent Psychiatry, Psychosomatics and Psychotherapy,

Ludwig-Maximilians-Universität, Munich, Germany

⁶ Department of Psychiatry, Massachusetts General Hospital, Harvard Medical School, Boston, USA

* - corresponding author

Email: p.wrobel@uke.de

- shared last authorship

Word count: Abstract: 250, Statement of significance: 118, Main text: 4249

Keywords: microstructure, cortex, DTI, specialization, aging

Figures: 2

30 **Significance statement**

31 Cortical thickness significantly contributed to systems neuroscience research related to cortical neuroplasticity. However,
32 regarding the underlying cortical microstructure it remains an unspecific measure. With a strong lateralization in diffusion
33 measures but not in thickness in specialized areas we demonstrate that cortical diffusion MRI is suitable to grasp
34 microstructural features linked to specialization already described in histology literature. The findings in the lateralization
35 of prefrontal and parietal cortical features may reflect age-related dynamic in cerebral activation. These results indicate the
36 great potential of cortical diffusion tensor imaging in neuroscience and may even emphasize a necessary paradigm shift
37 from the assessment of cortical macrostructure towards cortical microstructure for a better understanding of neuroplasticity
38 and structure-function relationships in health and disease.

39 **Abstract**

40
41 Characterizing cortical plasticity becomes increasingly important for identifying compensatory mechanisms and structural
42 reserve in the aging population. While cortical thickness (CT) largely contributed to systems neuroscience, it incompletely
43 informs about the underlying neuroplastic pathophysiology. In turn, microstructural characteristics may correspond to
44 atrophy mechanisms in a more sensitive way, indicating a potentially necessary paradigm shift in neuroimaging. Fractional
45 anisotropy (FA), a diffusion tensor imaging (DTI) measure, is inversely related to cortical histologic complexity. Axial
46 (AD) and radial diffusivity (RD) are assumed to be linked to density of structures oriented perpendicular and parallel to
47 cortical surface respectively. We hypothesized (1) that cortical DTI will reveal microstructural correlates for hemispheric
48 specialization, particularly in the language and motor systems and (2) that lateralization of cortical DTI parameters will
49 show an age effect, paralleling age-related changes in activation, especially in the prefrontal cortex. We re-analyzed data
50 of healthy younger and older adult participants (n=91). DTI measures and CT were extracted from Destrieux atlas regions.
51 Diffusion measures showed lateralization in specialized motor, language, visual, auditory, and inferior parietal cortices.
52 Age-dependent increased lateralization was observed for DTI measures in the prefrontal, angular, superior temporal, and
53 lateral occipital cortex. CT did not show any age-dependent alterations in lateralization. Our observations argue that cortical
54 DTI is able to capture correlates of microstructural properties associated with functional specialization, resembling findings
55 from histology. Age effects on diffusion measures in the integrative prefrontal and parietal areas may shed novel light on
56 the atrophy-related plasticity in healthy aging.

57 **Introduction**

58
59 The concept of hemispheric lateralization is a fundamental cerebral characteristic in systems neuroscience. Alterations in
60 lateralization have been shown to be altered depending on age with patterns of dedifferentiation (1-3). Findings that have
61 been contextualized by empirical models like the hemispheric asymmetry reduction in older adults (HAROLD) model (4-
62 9) can be observed primarily in the prefrontal cortex. However, cortical thickness (CT) appears to be limited for capturing
63 hemispheric specialization and poorly elucidates the mechanisms of its modulations. CT inconsistently reflects hemispheric
64 specialization of speech areas, which show a profound lateralization in functional studies (10-14). Moreover, one study on
65 a large dataset did not show any significant relationships between CT lateralization and age (15). The assumption that age
66 may lead to altered cortical lateralization appears reasonable as diffusion magnetic resonance imaging (MRI) data of the
67 white matter have already evidenced HAROLD-like reduced microstructural lateralization, particularly in the prefrontal
68 cortex (16, 17), coinciding with changes in glucose metabolism patterns (18). So far, the issue of cortical microscopic
69 correlates of brain plasticity in healthy aging has not been systematically explored by diffusion MRI (19).

70 Over a century ago Brodmann (20), Ramón y Cajal (21) and Vogt and Vogt (22) advocated the presence of inter-regional
71 diversity of cortical microstructure and thereby promoted fundamental concepts of specialization of the human brain (23).
72 Over time, imaging studies of structure-function and structure-behaviour relationships have continuously formed an
73 important area of research in fundamental and clinical neuroscience (24, 25). More recently, the aging population (26) has
74 led to an even greater interest in a better understanding of age-dependent changes in cortical structure and its relation to
75 functional and behavioural deterioration. The variability in cortical structural properties has been repeatedly related to
76 behavioural aspects in healthy aging, and to deficits and trajectories of recovery in neurological disease. The analysis of
77 CT, a surrogate of cortical macrostructure, dominates the field. However, the interpretation of CT and its integration with
78 brain function or behaviour is complicated as it is a relatively rough anatomic measure. CT sums multiple components
79 such as neurons, glia cells, extent of dendritic arborization, protein plaques and microangiopathy (27-31). In other words,
80 CT can tell us about the size of a structure while its complexity remains elusive.

81

82 Diffusion tensor imaging (DTI) has revolutionized the microstructural analyses of the brain. Primarily, it has been applied
83 to study white matter (32). However, technical progress, e.g., the introduction of free water correction (33), has increasingly
84 empowered DTI to capture cortical microstructural properties. Comparative studies on DTI and histology found an overlap
85 between tensors of both modalities, oriented orthogonally to the cortical surface due to columnar organization of neurons
86 (34). Fractional anisotropy (FA), used to measure the extent of directed tensor orientation, i.e., a surrogate of complexity
87 of cortical microstructure, was shown to decrease after birth as dendritic arborization in the cortex proceeds (35, 36). During
88 lifetime, cortical FA was then reported to show an increase in frontal areas in young and middle-aged adults suggesting a
89 decay in complexity of cortical microstructure (37), concurrent to synaptic pruning or neuronal degeneration. The
90 understanding to what extent the novel cortical DTI may be capable to capture fundamental characteristics of cortical
91 microanatomy is crucial to harness its potential.

92
93 Given the long-existing evidence for functional and microstructural hemispheric specialization and lateralization we first
94 hypothesized that diffusion-based surrogate parameters of cortical microstructure will be capable to capture lateralized
95 cortical features known from histology studies, particularly in the unimodal language and motor regions. Second, we
96 hypothesized to detect age-dependent changes in the amount of hemispheric lateralization, which we expected, particularly,
97 in heteromodal prefrontal cortices according to the HAROLD model. Following the interpretation of FA as a measure of
98 cortical microstructural complexity (35, 36), we assumed that directed water diffusion along the cortical columns, probably
99 representing the amount of neurons or afferent axons, would be best mapped by axial diffusivity (AD) whereas the diffusion
100 along structures parallel to the cortex, such as dendrites and interneurons, would be best captured by radial diffusivity (RD)
101 instead. To this end, we re-analyzed available imaging data of healthy younger and older adults from previously published
102 studies (38-42) using diffusion imaging to obtain cortical FA, AD, and RD values for 74 anatomic regions per hemisphere
103 and to infer the amount of hemispheric lateralization in these parameters. Lateralization patterns are reported for all
104 participants, group comparisons and interaction analyses were performed to assess differences between age groups.

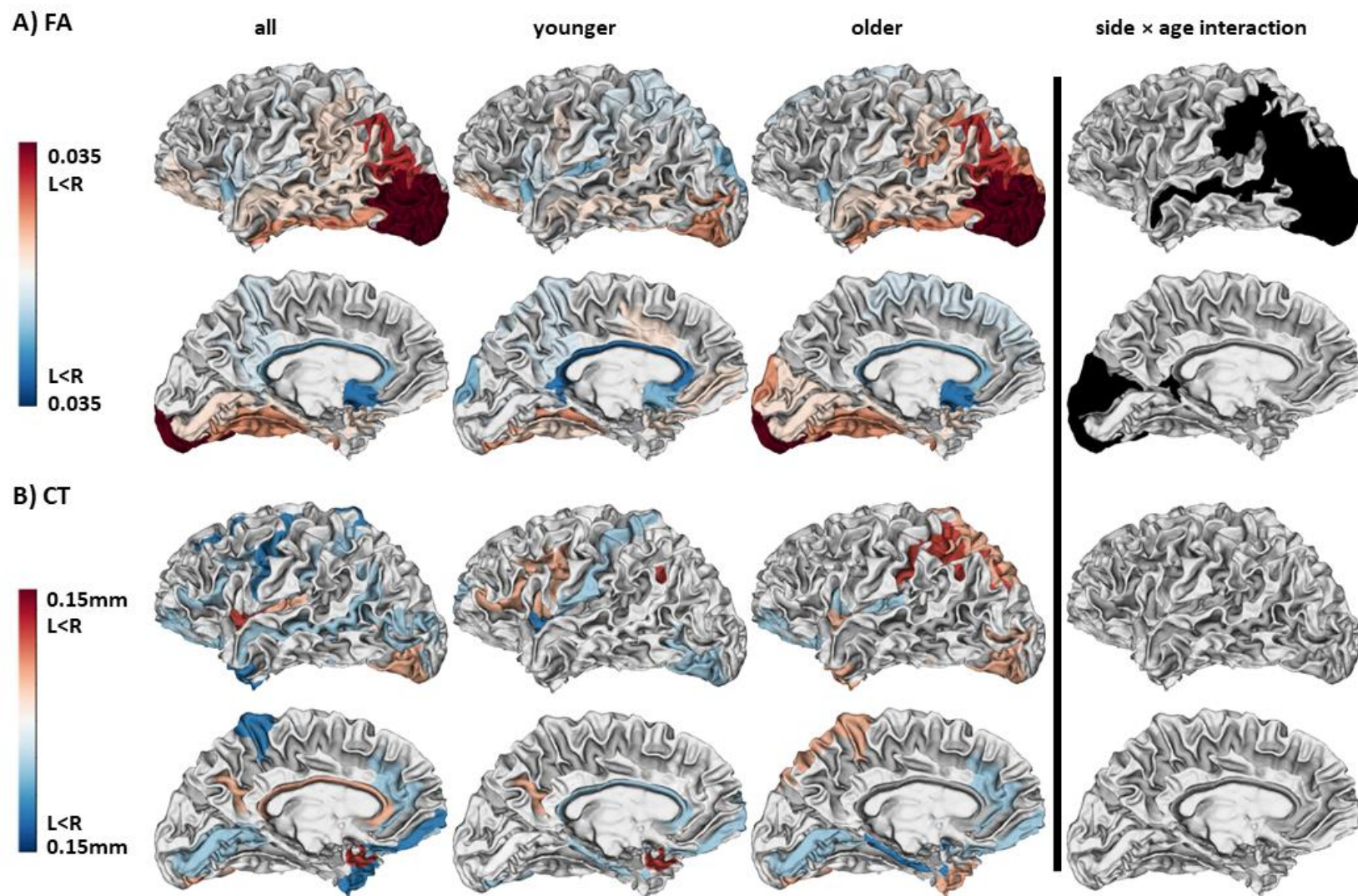
106 Results

107 Based on the association between the diffusion signal and cortical structure we calculated FA, AD, RD, and CT for 74
108 Destrieux atlas regions from imaging data of 43 younger and 48 older healthy right-handed adults. The assessment of
109 lateralization and its change with age was tested using linear mixed-effect models with side and age group covariates along
110 their interaction, while adjusting for the nuisance variables sex, study and, in case of diffusion measures, also CT value.
111 Figures 1 and 2 summarize the topography of regions exhibiting significant lateralization in cortical FA, AD, and RD,
112 respectively. CT measures are shown for comparative purposes.

113
114 In the combined group of younger and older adults, we found a lateralization with lower FA and AD in the dominant left
115 hemisphere in the planum temporale and higher FA in the triangular portion of the dominant inferior frontal gyrus, i.e.,
116 areas contributing to Wernicke's and Broca's areas. In the planum temporale, findings were driven by lower left
117 hemispheric AD in all groups, while RD was significantly greater in the left hemisphere only in younger adults. The
118 lateralized FA in the triangular inferior frontal gyrus was determined by an isolated FA finding with greater left-
119 hemispheric FA in younger adults. There were no significant interactions between lateralization and age group. CT did not
120 show any significant lateralization in regions contributing to Wernicke's and Broca's areas.

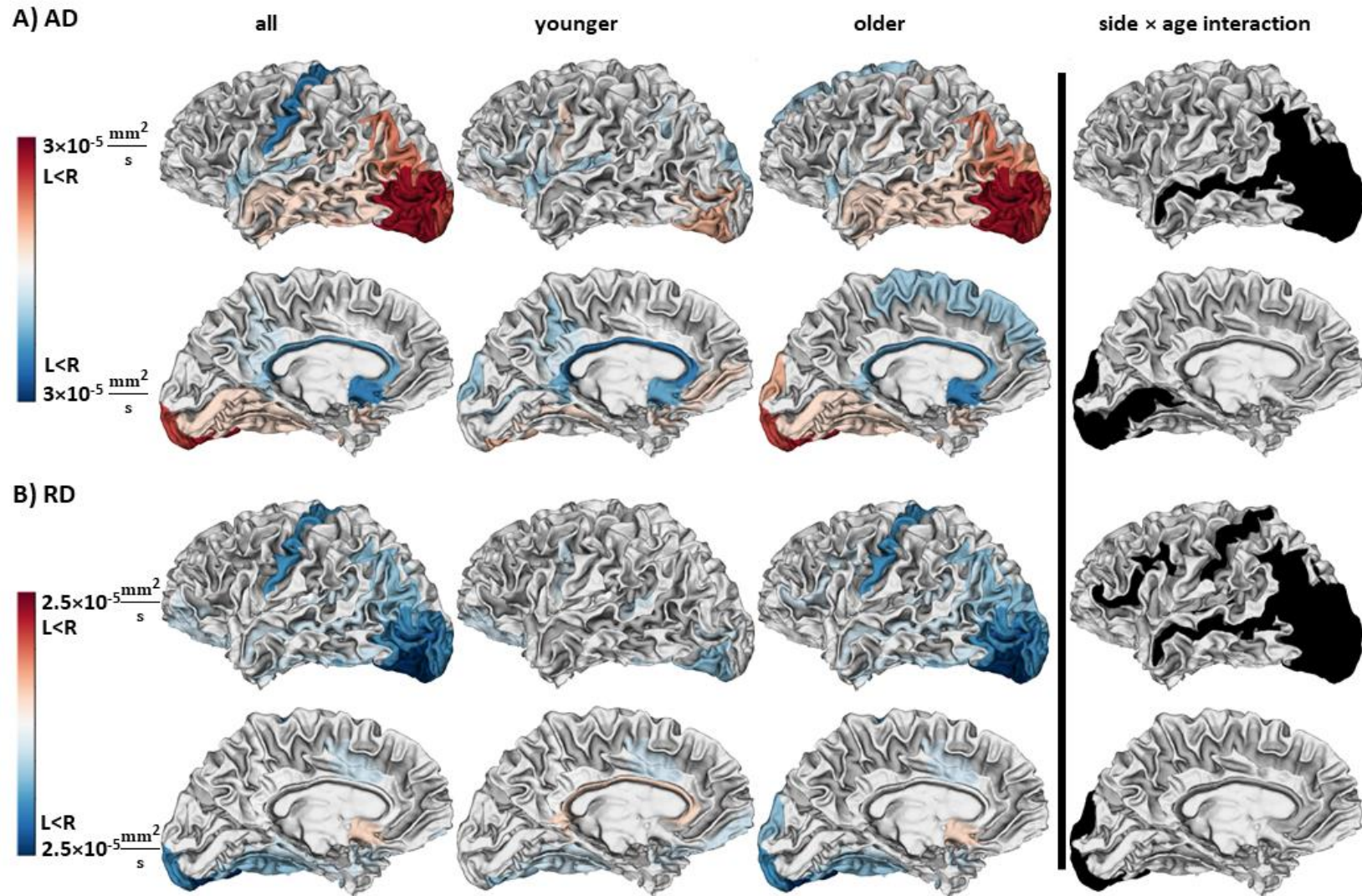
121
122 A significant lateralization was also detected in the precentral gyrus, which comprises the primary motor cortex, one of the
123 key areas of the human motor system. Here, we observed greater left hemispheric AD and RD but not FA in the combined
124 group. Notably, within-group analyses for younger and older participants revealed that RD was significantly greater in the
125 left hemisphere in older adults while AD showed a strong statistical trend towards a leftward lateralization (see Tables 1
126 and 2, Supporting Information). The younger adults did not show a significant lateralization in the precentral gyrus. Despite
127 this numerical group difference, interaction models could not evidence any significant age effects for the precentral gyrus.
128 There was no significant lateralization of CT in the precentral gyrus in any of the groups.

129



130
131
132
133
134

Figure 1 | Lateralization of fractional anisotropy (FA) and cortical thickness (CT) (red - left < right values, blue - left > right values) in the combined group of participants (column 1), in younger (column 2) and older participants (column 3) as well as regions with significant interaction between the age group and lateralization. Displayed are the color-coded differences between hemispheres. Detailed results can be found in Supplementary Tables 1 and 2.



135
136
137
138
139

Figure 2| Lateralization of axial (AD) and radial diffusivity (RD) (red - left < right values, blue – left > right values) in the combined group of participants (column 1), in younger (column 2) and older participants (column 3) as well as regions with significant interaction between the age group and lateralization. Displayed are the color-coded differences between hemispheres. Detailed results can be found in Supplementary Tables 1 and 2.

140 As examples for heteromodal brain areas, involved in motor and cognitive processes, hemispheric lateralization was also
141 detected in the angular part of the inferior parietal lobe which showed a greater FA and AD in the right hemisphere. Greater
142 RD was found in the left hemisphere in the combined group. The results were reproduced in the subgroup of older but not
143 younger adults. The intraparietal sulcus displayed similar patterns of lateralization in DTI measures. In contrast to the
144 language and motor areas, a statistically significant age effect was detected by interaction modeling in areas comprising
145 the angular and intraparietal sulcal cortex. Given the clustering around the angular gyrus, detailed plots for diffusivity
146 measures in both groups are provided in Supplementary Figure 3. Again, CT model yielded negative results also in these
147 areas.

148
149 We additionally observed a lateralization of DTI measures in the calcarine sulcus, which comprises the primary visual
150 cortex. However, greater left-hemispheric FA and AD were found only in younger adults.

151
152 We found age-dependent alterations in hemispheric microstructural asymmetry in prefrontal cortex in RD, but the greatest
153 number of regions with significant interactions was clustered at the temporo-parieto-occipital (TPO) junction for all
154 diffusion measures. There was no age-dependent lateralization in CT. As depicted in the images for sub-group analyses in
155 Figures 1 and 2 (columns 1 – 3), RD revealed an increase in leftward asymmetry in older adults in the prefrontal cortex
156 and the TPO cluster. AD and FA indicated greater values in the right hemisphere. A lateralization in these regions for
157 younger was observed solely for FA in the intraparietal sulcus (Figure 1, column 2).

158
159 In the temporal lobe, analyses of superior sulcus in the combined group and the older adults indicated that FA and AD
160 were associated with significantly lower left-hemispheric values. The RD showed relatively greater values in the left
161 hemisphere. An interaction with age group was also detected for all three DTI measures. The middle temporal and fusiform
162 gyri, the latter being associated with the visual word form area, showed lower leftward lateralization consistently across
163 all groups for FA, while a consistent finding was observed for RD in the fusiform cortex.

164 165 **Discussion**

166 The aim of this study was (1) to determine if diffusion-based surrogate parameters of cortical microstructure can detect
167 histological traits associated with hemispheric specialization and (2) to evaluate if the amount of hemispheric specialization
168 would show age-dependent changes. As the main findings we detected widespread lateralization of cortical microstructure,
169 operationalized by the diffusion parameters FA, RD, and AD, respectively, particularly in the inferior frontal, precentral,
170 superior, middle temporal, inferior parietal, and fusiform cortices. These cortices are not only part of language and motor
171 networks, but also of occipital visual and posterior parietal multimodal integrational brain networks. Age-dependent
172 increases in hemispheric lateralization were found primarily in the prefrontal cortex and in the temporo-parieto-occipital
173 junction cortices.

174 175 **Hemispheric lateralization in structure and function**

176 Based on comparative histology and DTI studies, we hypothesized to detect correlates of the structure-function relationship
177 in the fundamental concept of hemispheric lateralization. Cortical FA was assessed as a surrogate parameter for cortical
178 tissue complexity (34-36). Cortical AD was hypothesized to reflect the density of neurons, as these oblong structures
179 facilitate diffusion along tensors' main axis. Cortical RD was assumed to primarily correspond to structures facilitating
180 diffusion oriented in parallel to the cortical surface, such as dendrites and interneurons. We hypothesized that hemispheric
181 lateralization in these diffusion parameters would mirror hemispheric specialization, known from histology studies,
182 particularly for the language or motor systems. We identified five regions exhibiting pronounced hemispheric
183 specialization.

184
185 The first two regions were the planum temporale and the inferior frontal gyrus comprising Wernicke's and Broca's areas,
186 core regions of the human language network. In the planum temporale we observed lower left-hemispheric FA, which
187 could be induced by two different contributors. First, the accompanying reduction in left-hemispheric AD stands in line
188 with existing histology findings: Greater intercolumnar gaps between neurons with less oblong neurons compared to the
189 right-hemispheric homologue (43-45) can lead to smaller AD values and FA values on the left side. Second, denser and
190 more widespread dendritic arbors in the left planum temporale (46-48), extending to a certain degree parallel to the cortical
191 surface, might suggest a plausible link to the greater RD values observed in younger adults. Earlier studies proposed RD

192 to be inversely linked with neuron density due to the influence of myelination (49). Broca’s area (assessed via the triangular
193 inferior frontal cortex) has been characterized in a review by Keller *et al.* as poor in asymmetry on the macrostructural
194 level and showing microstructural lateralization “more often than not” (10). While previous microscopy studies have
195 reported multiple parameters to be lateralized in planum temporale, only a lower grey-level index (GLI) was observed for
196 Broca’s area (50, 51), suggesting lower fraction of perikaryal structures, which could be based on greater amount of
197 dendrites. One previous imaging study observed cortical microstructural lateralization for Wernicke’s area, but not for
198 Broca’s area (19). In the present analysis, we found greater FA values in the left Broca’s area driven by data from younger
199 adults. The link between cortical FA and the GLI remains speculative as the latter reflects the fraction of Nissl-stained
200 ribosomal structures, and not the number of neurons per se as glia cells would also contribute to GLI. Such cell populations
201 are less elongated, not as uniformly arranged as neurons in the cortex and highly different in cytomorphology. In contrast
202 to the planum temporale, due to absence of positive AD or RD findings it remains elusive if the difference in FA is driven
203 by differences in complexity or in density of axonal structures.

204

205 As a third region, greater AD and RD were measured in the left, dominant hemispheric precentral gyrus which comprises
206 the primary motor cortex. It was striking not to observe a lateralization of FA in the precentral area. However, given the
207 nature of FA as a ratio, even a more complex tissue may still show unchanged FA, if the amount of diffusivity along
208 neuronal columns remains relatively equal compared to the diffusion in the plane perpendicular to neuronal column’s axis.
209 This observation compels to evaluating cortical diffusion imaging in the light of diffusivity measures of AD and RD to
210 allow more precise statements on the microstructure. For instance, greater AD in the left and dominant motor cortex
211 indicates greater diffusivity perpendicular to cortical surface and could therefore corresponds to the neuronal density, which
212 was shown to be greater in the left primary motor cortex (52). In turn, a greater left RD (diffusivity parallel to the cortical
213 surface), significant only in older adults, could point towards a greater amount of dendritic or inter-neuronal structures.

214

215 Fourth, lateralization could be found beyond the eloquent areas of language and motor networks. Lower FA, AD, and
216 greater RD in the left-hemispheric inferior parietal cortex and the temporo-parieto-occipital junction could correspond to
217 specialization of the parietal cortex in higher-order integrative functions that was observed in imaging and stimulation
218 studies (8, 53), while ischemic lesions affecting right inferior parietal cortices have been linked with neglect and apraxia
219 (54, 55). Strikingly, one would expect greater AD and RD, in particular when considering the specialization, in the right
220 hemisphere as these could represent greater neuronal count and dendritic arborization or interneuronal density in the
221 specialized area. However, as the visualized data for the angular gyrus from both subgroups suggest (see Supplementary
222 Figure 3), the lateralization of AD and RD becomes apparent in late adulthood. Concurrently, the absolute level of AD is
223 greater and the absolute level of RD is lower in the older group, which could correspond to a greater axonal density and
224 lower dendritic axonal complexity, induced by reduction of non-axonal structures along a constant amount of neurons.
225 This is in line with earlier descriptions in review literature (56).

226

227 Fifth, the observed lateralization of the visual system in younger adults was a striking finding. Even though there are single
228 reports on interhemispheric differences in activity of the calcarine cortex (9), the literature on this topic is sparse compared
229 to data on asymmetry in motor and language function. Future studies will have to confirm this result.

230

231 Taken together, the number, the topography, and the side specificity in lateralization of cortical DTI measures encourage
232 viewing these as a promising surrogate for functional hemispheric specialization. For instance, the RD findings appear to
233 resemble histological findings on dendritic arborization in the planum temporale (43, 47) while AD lateralization
234 corresponds with findings on neuronal/axonal density in the planum temporale (43, 57), the fusiform cortex (58) and the
235 inferior parietal lobe (59). This agreement of lateralized cortical DTI metrics and classical histology supports the view that
236 DTI is able to capture cortical microstructural traits which remain hidden for CT based morphometric analyses in the motor
237 or language network. The absence of a positive finding for CT compared to the results of Kong *et al.* could rely on the
238 larger sample size ($n > 17000$) which indicates that surrogates for microstructure could be not only more specific but also
239 more sensitive (15).

240

241 **Influence of age on microstructural hemispheric specialization**

242 Our second hypothesis was that cortical DTI metrics are able to detect age-dependent changes in hemispheric lateralization.

243 Multiple functional MRI and EEG studies have shown alterations in hemispheric activation with age, particularly in
244 prefrontal cortices which has been contextualized with theoretical models such as the HAROLD model (4, 60). Reduction
245 in hemispheric asymmetry of functional activity in older adults (i.e. the HAROLD model) has been argued to reflect
246 compensatory mechanisms to overcome a decline in cortical integrative function (9). In this study, the inferior frontal sulcal
247 and the inferior parietal cortex, two heteromodal integrative areas, displayed an age-dependent increase in lateralization
248 due to a stronger right-hemispheric lateralization in absolute measures (Figures 1 and 2 – fourth column, Supplementary
249 Figure 3). Such dynamic of lateralization towards the opposite hemisphere is highly suggestive for a reorganization that
250 might be linked to compensatory activity. From a clinical perspective, the distribution of significant findings in the inferior
251 parietal cortex would be in line with the assumption that cortical aging and degenerative disorders primarily affect higher
252 cognitive and integrational processes due to subtle reorganization rather than the function of primary areas (61). Even
253 though the second hypothesis appears to be confirmed considering the finding of lateralized RD in prefrontal
254 microstructure, the results' distribution (Figures 1 and 2 - fourth column), is highly suggestive that age-dependent
255 organization is more strongly pronounced in posterior brain regions. Besides the HAROLD model, aging-related processes
256 have been proposed to show a posterior to anterior shift, contextualized by the PASA model (62). The findings in the TPO
257 cluster in this study seem to support the assumption of this shift, which has already been discussed by Rathi *et al.* in
258 analyses on DTI measures on a gross, lobar level (37).

259 Of note, the focus on structure in this study allows only speculative judgements on the underlying mechanisms. The
260 morphology of the aging cortex has been characterized by distinct and focal changes in dendritic branching rather than by
261 extensive neuronal loss (56), which would be primarily reflected by a reduction of RD and to lesser extent also in FA. Such
262 reorganization would unlikely cause reorganization measured by AD. However, an altered diffusion along the neuronal
263 columns may be also explained by altered afferent fibers resulting from white matter lesions leading to a disconnection
264 syndromes due to Wallerian degeneration (16, 17). An earlier study of our group showed that better performing older adults
265 show a greater white matter integrity, operationalized by regional FA, compared to low performing peers (39). Again,
266 cortical DTI measures, grasping such nuances based on single-shell imaging, appear to be superior to CT based
267 measurements (15).

268

269 **Implications**

270 Cortical DTI with apparent advantages over CT bears a great potential for future clinical research questions. Current
271 implications primarily focus on diagnostics. The observed relationship between AD and neuronal density as well as
272 between RD and dendritic arborization may encourage researchers to further promote the usage of cortical DTI to address
273 potential cortical microstructural alterations in neurological diseases (63). Furthermore, a better characterization of
274 temporal and spatial aspects of neuroplasticity could reveal targets for stimulation techniques, secondarily improving their
275 efficacy and efficiency.

276

277 **Methodical limitations**

278 There are several important limitations to note: First, five different studies were re-analyzed in this work. We controlled
279 our models for study category, despite the acquisition on the same scanner. The inconsistent T1-data resolution in two
280 studies is unlikely to confound the results as it had to be downgraded to the resolution of the diffusion data prior to DTI
281 measure estimation. Second, the study does not allow a lifespan analysis due to the cross-sectional character, indicating
282 the necessity to verify our observations in a longitudinal dataset. Third, beside absent information on education and
283 socioeconomic background the behavioral data of some studies lacked standardized handedness testing such as the
284 Edinburgh Handedness Inventory. Instead, the participants had to declare their handedness, which could potentially lead
285 to inclusion of participants trained to right-handedness. Fourth, the diffusion image resolution was 2mm, this might be
286 rather lower when aiming to assess cortical microstructure. However, given the strong differences observed in a
287 conservative analysis and standing in line with existing histology reports, we consider the results as robust. Nevertheless,
288 cortical DTI analyses should be further improved using high-resolution protocols in the future. Fifth, due to existing but
289 still sparse literature it is challenging to compare the absolute DTI measures results to other studies. Even though we could
290 reproduce insular cortex values known from previous studies (64), future work must validate our results. Differences in
291 scanners, resolution of MRI datasets and different approaches of preprocessing might influence cortical DTI metrics.
292 However, we assume that measuring lateralization, in which every participant serves as his or her own control, sufficiently
293 accounts for this limitation.

294

295 **Conclusion**

296 Cortical DTI measures unambiguously grasped microstructural hemispheric lateralization in core areas known for
297 asymmetry in function such as the motor and language networks, with FA showing different degree of variation between
298 areas of higher and lower integrative function. This work further demonstrated age-related reorganization processes in
299 integrative heteromodal, secondary cortices, which corresponds to findings from studies on cerebral activity. From a
300 methodical perspective the present findings indicate, that (1) cortical DTI grasps not only myelinated structures within
301 white matter but also the complexity from non-myelinated tissue in the cortical gray matter and (2) the diffusivity measures
302 AD and RD may reflect specific histoarchitectural traits, such as neuronal density and dendritic arborization, being
303 therefore compulsory for interpretation of FA in the cerebral cortex.

304

305 **Materials and methods**

306

307 **Participants Data**

308 Imaging and clinical data were screened from five individual datasets contributing to studies which have previously been
309 published by our laboratory (38-42). Datasets of healthy right-handed participants within two age-ranges (18-30 and 60-
310 87 years) with sufficient data quality were included in this secondary analysis. In total, 91 of initially 123 datasets were
311 analyzed (number of included datasets from each study - Study A (38): 14 of 23 [older adults], Study B (39): 39 of 50 [19
312 younger and 20 older adults], Study C (40): 18 of 20 [younger adults], Study D (41): 8 of 13 [6 younger and 2 older adults],
313 Study E (42): 12 of 17 [older adults]). The exclusions were based on age beyond the range of interest and data quality. In
314 sum, age groups consisted of 43 younger (mean 24.4 years, standard deviation [SD] 2.5, range 18-30, 26 female) and 48
315 older participants (mean 71.7 years, SD 6.0, range 60-87, 22 female). Brain imaging for all participants had been conducted
316 on the same MRI scanner. The original studies were conducted following the Declaration of Helsinki and approved by the
317 local ethics committee of the Medical Association of Hamburg. All participants gave written informed consent.

318

319 **Brain Imaging and Processing**

320 All participants were scanned on a 3 Tesla Siemens Skyra Scanner (Siemens Healthineers, Erlangen, Germany) with a 32-
321 channel head coil. T1-weighted imaging was based on a magnetization-prepared, rapid acquisition gradient-echo sequence
322 (MPRAGE) (repetition time (TR) = 2.500ms, echo time (TE) = 2.12ms, 256 slices with a field of view (FOV) =
323 240x192mm, interslice distance of 0.94mm and an in-plane resolution range between 0.94x0.94mm and 0.83x0.83mm).
324 DTI datasets were consistent in imaging parameters, with 75 slices in 64 non-collinear gradient directions with a b-value
325 of 1500s/mm² as well as one b₀ image (FOV = 208 × 256 mm², flip angle = 90°, TE = 82ms, TR = 10000ms and voxel size
326 of 2x2x2mm). Each individual dataset underwent manual quality check excluding datasets with motion artifacts, for
327 instance ringing, ghosting or tissue cuts, leading to insufficient reconstruction of grey and white matter boundary, and
328 datasets with cerebral tissue outside the FOV.

329 T1-weighted images were segmented into 74 cortical anatomic regions per hemisphere from the Destrieux atlas (65) using
330 the FreeSurfer based *recon-all* tool (version 6.0.1) (66) yielding CT values and individual labels for identification of regions
331 in DTI data. The data was post-processed and registered to the individual pre-processed DTI using Advanced
332 Normalization Tools (ANTs 2.3.4) (67) while adjusting the resolution to 2x2x2mm. DTI datasets were corrected for eddy
333 currents using MRtrix3 (3.0.2) tools based on the FSL (6.0.1) correction method (68, 69). Distortion correction was applied
334 by registering the b₀-weighted diffusion image to the T1-weighted image using ANTs, MRTrix3 and FSL. For free water
335 (FW) correction of the cortical DTI signals, a custom written MATLAB script was used (ran on Matlab R2020a, The
336 Mathworks, Natick, MA, USA). In brief, a bi-tensor model with a fixed diffusivity for FW and a second representing water
337 diffusion in presence of tissue membranes (33) was fitted and mean FA, AD and RD values were derived from FW-
338 corrected tensor eigenvalues for each cortical area.

339

340 **Statistical Analysis**

341 Statistics were performed using R software version 4.0.2 (70). Linear mixed-effects models with repeated measures were
342 fitted to describe the extent of label-wise hemispheric lateralization in cortical microstructure. Specifically, in separate
343 models for FA, AD, RD, and CT in all participants (N=91), mean absolute values were treated as the dependent variable
344 (DV), SIDE (left, right) was treated as the independent variable of interest. Target effects were adjusted in a multivariate
345 approach for the nuisance variables AGE_GROUP, AGE_GROUP × SIDE interaction, STUDY, SEX, as well as CT in
346 models for diffusion measures. The necessity to adjust for CT is explained in the supplementary text 1, see Supporting

347 Information. The amount of hemispheric lateralization is based on the coefficient SIDE (mean difference between
348 hemispheres), its statistical significance (P_{SIDE}) is fully corrected for multiple comparisons using the false discovery rate
349 (FDR) method for 74 Destrieux atlas regions per DTI parameter. The age-dependent change of lateralization is based on
350 the coefficient AGE_GROUP \times SIDE, its statistical significance ($P_{\text{AGE_GROUP} \times \text{SIDE}}$) was corrected in the same manner as
351 the SIDE effect. To specifically address age effects, separate models were also fitted for the younger (N=43) and older
352 (N=48) participants separately, with AGE as covariate. Statistical significance was assumed at corrected $P_{\text{FDR}} < 0.05$. Brain
353 illustrations were generated using the *fsbrain* package in R.

354 **Acknowledgments and funding:** This work was supported by the German Research Foundation (DFG) and the National
355 Science Foundation of China (NSFC) in project Crossmodal Learning, TRR-169/A3 (C.G.), the Deutsche
356 Forschungsgemeinschaft (DFG, German Research Foundation) – SFB936-178316478 - C1 (C.G.) & C2 (G.T., B.C.),
357 Werner Otto Stiftung (4/90, R.S.), Else Kröner-Fresenius-Stiftung (grant numbers 2020_EKES.16, R.S.).

358
359

360 Bibliography

361

- 362 1. K. Cassady, M. F. L. Ruitenbergh, P. A. Reuter-Lorenz, M. Tommerdahl, R. D. Seidler, Neural Dedifferentiation
363 across the Lifespan in the Motor and Somatosensory Systems. *Cereb Cortex* **30**, 3704-3716 (2020).
- 364 2. J. Carp, J. Park, A. Hebrank, D. C. Park, T. A. Polk, Age-related neural dedifferentiation in the motor system.
365 *PLoS One* **6**, e29411 (2011).
- 366 3. F. Quandt *et al.*, Spectral Variability in the Aged Brain during Fine Motor Control. *Front Aging Neurosci* **8**, 305
367 (2016).
- 368 4. R. Cabeza, Hemispheric asymmetry reduction in older adults: The HAROLD model. *Psychology and Aging* **17**,
369 85-100 (2002).
- 370 5. F. Dolcos, H. J. Rice, R. Cabeza, Hemispheric asymmetry and aging: right hemisphere decline or asymmetry
371 reduction. *Neurosci Biobehav Rev* **26**, 819-825 (2002).
- 372 6. M. Esteves *et al.*, Structural laterality is associated with cognitive and mood outcomes: An assessment of 105
373 healthy aged volunteers. *Neuroimage* **153**, 86-96 (2017).
- 374 7. T. Guadalupe *et al.*, Human subcortical brain asymmetries in 15,847 people worldwide reveal effects of age and
375 sex. *Brain Imaging Behav* **11**, 1497-1514 (2017).
- 376 8. K. Caeyenberghs, A. Leemans, Hemispheric lateralization of topological organization in structural brain networks.
377 *Hum Brain Mapp* **35**, 4944-4957 (2014).
- 378 9. M. Berlinger, L. Danelli, G. Bottini, M. Sberna, E. Paulesu, Reassessing the HAROLD model: is the hemispheric
379 asymmetry reduction in older adults a special case of compensatory-related utilisation of neural circuits? *Exp*
380 *Brain Res* **224**, 393-410 (2013).
- 381 10. S. S. Keller, T. Crow, A. Foundas, K. Amunts, N. Roberts, Broca's area: Nomenclature, anatomy, typology and
382 asymmetry. *Brain and Language* **109**, 29-48 (2009).
- 383 11. D. N. Greve *et al.*, A surface-based analysis of language lateralization and cortical asymmetry. *J Cogn Neurosci*
384 **25**, 1477-1492 (2013).
- 385 12. R. Dorsaint-Pierre *et al.*, Asymmetries of the planum temporale and Heschl's gyrus: relationship to language
386 lateralization. *Brain* **129**, 1164-1176 (2006).
- 387 13. D. Zhou, C. Lebel, A. Evans, C. Beaulieu, Cortical thickness asymmetry from childhood to older adulthood.
388 *Neuroimage* **83**, 66-74 (2013).
- 389 14. K. J. Plessen, K. Hugdahl, R. Bansal, X. Hao, B. S. Peterson, Sex, age, and cognitive correlates of asymmetries in
390 thickness of the cortical mantle across the life span. *J Neurosci* **34**, 6294-6302 (2014).
- 391 15. X. Z. Kong *et al.*, Mapping cortical brain asymmetry in 17,141 healthy individuals worldwide via the ENIGMA
392 Consortium. *Proc Natl Acad Sci U S A* **115**, E5154-E5163 (2018).
- 393 16. A. Pfefferbaum, E. Adalsteinsson, E. V. Sullivan, Frontal circuitry degradation marks healthy adult aging:
394 Evidence from diffusion tensor imaging. *NeuroImage* **26**, 891-899 (2005).
- 395 17. Z. Li, A. B. Moore, C. Tyner, X. Hu, Asymmetric connectivity reduction and its relationship to "HAROLD" in
396 aging brain. *Brain Research* **1295**, 149-158 (2009).
- 397 18. P. A. Reuter-Lorenz *et al.*, Age differences in the frontal lateralization of verbal and spatial working memory
398 revealed by PET. *J Cogn Neurosci* **12**, 174-187 (2000).
- 399 19. J. Schmitz *et al.*, Hemispheric asymmetries in cortical gray matter microstructure identified by neurite orientation
400 dispersion and density imaging. *NeuroImage* **189**, 667-675 (2019).
- 401 20. K. Brodmann, *Vergleichende Lokalisationslehre der Großhirnrinde in ihren Prinzipien dargestellt auf Grund des*
402 *Zellenbaues* (J.A. Barth, Leipzig, 1909).
- 403 21. S. Ramón y Cajal, *Histologie Du Système Nerveux de l'Homme Et Des Vertébrés* (Paris, 1909).

- 404 22. C. V. Vogt, O., Allgemeinere Ergebnisse unserer Hirnforschung. *J.f. Psychologie und Neurologie*, 279–468
405 (1919).
- 406 23. P. Broca, Sur le siège de la faculté du langage articulé. *Bulletins et Mémoires de la Société d'Anthropologie de*
407 *Paris*, 377-393 (1865).
- 408 24. B. Fischl, A. M. Dale, Measuring the thickness of the human cerebral cortex from magnetic resonance images.
409 *Proceedings of the National Academy of Sciences* **97**, 11050-11055 (2000).
- 410 25. S. M. Smith *et al.*, Tract-based spatial statistics: voxelwise analysis of multi-subject diffusion data. *Neuroimage*
411 **31**, 1487-1505 (2006).
- 412 26. R. Brookmeyer, S. Gray, C. Kawas, Projections of Alzheimer's disease in the United States and the public health
413 impact of delaying disease onset. *Am J Public Health* **88**, 1337-1342 (1998).
- 414 27. D. P. Pelvig, H. Pakkenberg, A. K. Stark, B. Pakkenberg, Neocortical glial cell numbers in human brains.
415 *Neurobiology of Aging* **29**, 1754-1762 (2008).
- 416 28. F. A. C. Azevedo *et al.*, Equal numbers of neuronal and nonneuronal cells make the human brain an isometrically
417 scaled-up primate brain. *The Journal of Comparative Neurology* **513**, 532-541 (2009).
- 418 29. Z. Petanjek *et al.*, Extraordinary neoteny of synaptic spines in the human prefrontal cortex. *Proceedings of the*
419 *National Academy of Sciences* **108**, 13281-13286 (2011).
- 420 30. A. Biller *et al.*, Responses of the Human Brain to Mild Dehydration and Rehydration Explored In Vivo by
421 ¹H-MR Imaging and Spectroscopy. *American Journal of Neuroradiology* **36**, 2277-2284 (2015).
- 422 31. J. Shin *et al.*, Cell-Specific Gene-Expression Profiles and Cortical Thickness in the Human Brain. *Cerebral*
423 *Cortex* **28**, 3267-3277 (2018).
- 424 32. P. J. Basser, C. Pierpaoli, Microstructural and physiological features of tissues elucidated by quantitative-
425 diffusion-tensor MRI. *J Magn Reson B* **111**, 209-219 (1996).
- 426 33. O. Pasternak, N. Sochen, Y. Gur, N. Intrator, Y. Assaf, Free water elimination and mapping from diffusion MRI.
427 *Magn Reson Med* **62**, 717-730 (2009).
- 428 34. S. N. Jespersen, L. A. Leigland, A. Cornea, C. D. Kroenke, Determination of axonal and dendritic orientation
429 distributions within the developing cerebral cortex by diffusion tensor imaging. *IEEE Trans Med Imaging* **31**, 16-
430 32 (2012).
- 431 35. C. D. Kroenke, E. N. Taber, L. A. Leigland, A. K. Knutsen, P. V. Bayly, Regional patterns of cerebral cortical
432 differentiation determined by diffusion tensor MRI. *Cereb Cortex* **19**, 2916-2929 (2009).
- 433 36. C. D. Kroenke, Using diffusion anisotropy to study cerebral cortical gray matter development. *J Magn Reson* **292**,
434 106-116 (2018).
- 435 37. Y. Rathi *et al.*, Gray matter alterations in early aging: a diffusion magnetic resonance imaging study. *Hum Brain*
436 *Mapp* **35**, 3841-3856 (2014).
- 437 38. E. Schlemm *et al.*, Structural brain networks and functional motor outcome after stroke-a prospective cohort
438 study. *Brain Commun* **2**, fcaa001 (2020).
- 439 39. F. L. Higgen *et al.*, Reduced frontal white matter microstructure in healthy older adults with low tactile
440 recognition performance. *Scientific Reports* **11**, 11689-11689 (2021).
- 441 40. R. Schulz *et al.*, White Matter Integrity of Specific Dentato-Thalamo-Cortical Pathways is Associated with
442 Learning Gains in Precise Movement Timing. *Cereb Cortex* **25**, 1707-1714 (2015).
- 443 41. M. Zimmerman *et al.*, Impairment of Procedural Learning and Motor Intracortical Inhibition in Neurofibromatosis
444 Type 1 Patients. *EBioMedicine* **2**, 1430-1437 (2015).
- 445 42. S. Guder *et al.*, The Influence of Cortico-Cerebellar Structural Connectivity on Cortical Excitability in Chronic
446 Stroke. *Cereb Cortex* **30**, 1330-1344 (2020).
- 447 43. H. L. Seldon (1981) STRUCTURE OF HUMAN AUDITORY CORTEX. I. CYTOARCHITECTONICS AND
448 DENDRITIC DISTRIBUTIONS. in *Brain Research*, pp 277-294.
- 449 44. S. A. Chance, M. F. Casanova, A. E. Switala, T. J. Crow, Minicolumnar structure in Heschl's gyrus and planum
450 temporale: Asymmetries in relation to sex and callosal fiber number. *Neuroscience* **143**, 1041-1050 (2006).
- 451 45. R. A. W. Galuske, W. Schlote, H. r. Bratzke, W. Singer, Interhemispheric Asymmetries of the Modular Structure
452 in Human Temporal Cortex. *Science* **289**, 1946-1949 (2000).
- 453 46. E. Di Rosa, T. J. Crow, M. A. Walker, G. Black, S. A. Chance, Reduced neuron density, enlarged minicolumn
454 spacing and altered ageing effects in fusiform cortex in schizophrenia. *Psychiatry Research* **166**, 102-115 (2009).
- 455 47. H. L. Seldon (1982) Structure of Human Auditory Cortex. III. Statistical Analysis of Dendritic Trees. in *Brain*
456 *Research*, pp 211-221.
- 457 48. B. Jacobs, M. Schall, A. B. Scheibel, A quantitative dendritic analysis of Wernicke's area in humans. II. Gender,
458 hemispheric, and environmental factors. *J Comp Neurol* **327**, 97-111 (1993).
- 459 49. C. Reveley *et al.*, Diffusion MRI anisotropy in the cerebral cortex is determined by unmyelinated tissue features.
460 *Nat Commun* **13**, 6702 (2022).
- 461 50. K. Amunts *et al.*, Broca's region revisited: Cytoarchitecture and intersubject variability. *The Journal of*
462 *Comparative Neurology* **412**, 319-341 (1999).

- 463 51. K. Amunts, A. Schleicher, A. Ditterich, K. Zilles, Broca's region: Cytoarchitectonic asymmetry and
464 developmental changes. *The Journal of Comparative Neurology* **465**, 72-89 (2003).
- 465 52. C. C. Sherwood, E. Wahl, J. M. Erwin, P. R. Hof, W. D. Hopkins, Histological asymmetries of primary motor
466 cortex predict handedness in chimpanzees (Pan troglodytes). *J Comp Neurol* **503**, 525-537 (2007).
- 467 53. J. Misselhorn *et al.*, Sensory capability and information integration independently explain the cognitive status of
468 healthy older adults. *Sci Rep* **10**, 22437 (2020).
- 469 54. T. Hamano, S. Kimura, S. Miyao, J. Teramoto, Apraxia of eyelid closure complicating right parietal infarction.
470 *Eur Neurol* **45**, 122-123 (2001).
- 471 55. J. D. Pandian *et al.*, Mirror therapy in unilateral neglect after stroke (MUST trial): a randomized controlled trial.
472 *Neurology* **83**, 1012-1017 (2014).
- 473 56. S. N. Burke, C. A. Barnes, Neural plasticity in the ageing brain. *Nat Rev Neurosci* **7**, 30-40 (2006).
- 474 57. J. F. Smiley *et al.*, Hemispheric comparisons of neuron density in the planum temporale of schizophrenia and
475 nonpsychiatric brains. *Psychiatry Research - Neuroimaging* **192**, 1-11 (2011).
- 476 58. S. A. Chance *et al.*, Hemispheric asymmetry in the fusiform gyrus distinguishes Homo sapiens from chimpanzees.
477 *Brain Structure and Function* **218**, 1391-1405 (2013).
- 478 59. J. F. Smiley, K. Konnova, C. Bleiwas, Cortical thickness, neuron density and size in the inferior parietal lobe in
479 schizophrenia. *Schizophrenia Research* **136**, 43-50 (2012).
- 480 60. T. J. Bellis, T. Nicol, N. Kraus, Aging affects hemispheric asymmetry in the neural representation of speech
481 sounds. *J Neurosci* **20**, 791-797 (2000).
- 482 61. R. Mielke *et al.*, Normal and pathological aging--findings of positron-emission-tomography. *J Neural Transm*
483 *(Vienna)* **105**, 821-837 (1998).
- 484 62. S. W. Davis, N. A. Dennis, S. M. Daselaar, M. S. Fleck, R. Cabeza, Que PASA? The Posterior-Anterior Shift in
485 Aging. *Cerebral Cortex* **18**, 1201-1209 (2008).
- 486 63. V. L. Villemagne, V. Dore, S. C. Burnham, C. L. Masters, C. C. Rowe, Imaging tau and amyloid-beta
487 proteinopathies in Alzheimer disease and other conditions. *Nat Rev Neurol* **14**, 225-236 (2018).
- 488 64. R. P. Cabeen, A. W. Toga, J. M. Allman, Mapping fronto-insular cortex from diffusion microstructure. *Cereb*
489 *Cortex* **33**, 2715-2733 (2023).
- 490 65. C. Destrieux, B. Fischl, A. Dale, E. Halgren, Automatic parcellation of human cortical gyri and sulci using
491 standard anatomical nomenclature. *Neuroimage* **53**, 1-15 (2010).
- 492 66. B. Fischl *et al.*, Automatically parcellating the human cerebral cortex. *Cereb Cortex* **14**, 11-22 (2004).
- 493 67. B. B. Avants *et al.*, A reproducible evaluation of ANTs similarity metric performance in brain image registration.
494 *NeuroImage* **54**, 2033-2044 (2011).
- 495 68. M. Jenkinson, C. F. Beckmann, T. E. Behrens, M. W. Woolrich, S. M. Smith, Fsl. *Neuroimage* **62**, 782-790
496 (2012).
- 497 69. J. D. Tournier *et al.*, MRtrix3: A fast, flexible and open software framework for medical image processing and
498 visualisation. *Neuroimage* **202**, 116137 (2019).
- 499 70. R_Core_Team (2008) R: A language and environment for statistical computing. (R Foundation for Statistical
500 Computing, Vienna, Austria).